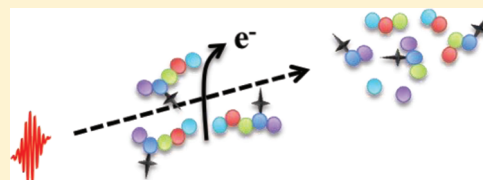


Mechanism Elucidation for Nonstochastic Femtosecond Laser-Induced Ionization/Dissociation: From Amino Acids to Peptides

Christine L. Kalcic,[†] Gavin E. Reid,^{†,‡} Vadim V. Lozovoy,[†] and Marcos Dantus^{*,†,§}[†]Departments of Chemistry, [‡]Biochemistry and Molecular Biology, and [§]Physics and Astronomy, Michigan State University East Lansing, Michigan 48824, United States

ABSTRACT: Femtosecond laser-induced ionization/dissociation (fs-LID) has been demonstrated as a novel ion activation method for use in tandem mass spectrometry. The technique opens the door to unique structural information about biomolecular samples that is not easily accessed by traditional means. fs-LID is able to cleave strong bonds while keeping weaker bonds intact. This feature has been found to be particularly useful for the mapping of post-translational modifications such as phosphorylation, which is difficult to achieve by conventional proteomic studies. Here we investigate the laser–ion interaction on a fundamental level through the characterization of fs-LID spectra for the protonated amino acids and two series of derivatized samples. The findings are used to better understand the fs-LID spectra of synthetic peptides. This is accomplished by exploring the effects of several single-residue substitutions.



1. INTRODUCTION

With the development of soft ionization methods such as electrospray ionization (ESI) and matrix-assisted laser desorption/ionization (MALDI), which yield intact pseudomolecular ions,^{1,2} tandem mass spectrometry has become a robust tool for the interrogation of molecular structure in the gas phase. More specifically, high-throughput capabilities are routinely used in the field of proteomics to analyze thousands of peptides in an efficient manner. In a typical MS/MS experiment, a magnetic or electric field is used to isolate a precursor ion of interest from the bulk of the sample, and this precursor ion population is then activated, leading to dissociation into a series of product ions that are detected in the MS/MS spectrum.³ If a different ion activation method is employed, it may promote dissociation of the precursor ions along a different pathway, leading to a complementary MS/MS spectrum of product ions.⁴ A researcher can either analyze this spectrum by hand or use computer software to map out the most likely structure of the original precursor ion. When an ion activation method is capable of breaking more bonds within a molecule, the MS/MS spectrum contains a greater number of overlapping product ions, and the original structure of the analyte can be determined more completely and with greater confidence. For any given peptide sample, the ion activation method employed must be capable of generating sufficient product ions for unambiguous sequencing and mapping of structural modifications.⁵ Structure determination can become problematic if certain regions in a peptide resist fragmentation. In some cases it is important to preserve weakly bound peptide modifications, while cleaving the stronger peptide bonds. To find a solution to these challenges, there is great interest in the development and characterization of new ion activation methods. Each method serves as an additional tool for tandem mass spectrometry experiments.

Femtosecond laser-induced ionization/dissociation (fs-LID) is one such alternative ion activation method, recently developed in the Dantus and Reid groups. The technique couples ultrafast

near-IR laser irradiation with the MSⁿ capability of an ion trap mass spectrometer. The fs-LID instrumentation and method were first described in 2009, and the technique was demonstrated to cause extensive dissociation of four peptides, including singly, doubly, and triply protonated species, resulting in the formation of numerous product ions from which the sequence could be readily determined.⁶ It was found that fs-LID is most efficient for singly protonated precursor ions, which is consistent with the estimate that ionization energy of peptides increases approximately 1.1 eV with each additional positive charge.⁷ This study also illustrated the utility of fs-LID for the mapping of labile post-translational modifications along the peptide chain. Phosphorylation is one of the most important types of protein modifications, as it typically plays the role of enzyme activation or inhibition. The ability to map phosphorylation was tested using two model synthetic phosphothreonine containing peptides. The femtosecond time-scale activation proved of importance both for the ultrafast creation of the radical cation and for the ultrafast cleavage of chemical bonds occurring at a rate faster than intramolecular energy redistribution. The applicability of fs-LID to phosphopeptide analysis was investigated further for singly protonated phosphopeptides.⁸ Radical-driven sequence ions (a, c, x, and z ions) were observed for all six of the peptides studied, and there was no dominant phosphate loss or phosphate group scrambling. Additionally, fs-LID provided diagnostic product ions for the unambiguous characterization of phosphorylation sites.⁸ fs-LID has also been used for the analysis of protonated biomolecules other than peptides. The method works to dissociate fatty acid chains in

Special Issue: Femto10: The Madrid Conference on Femtochemistry

Received: August 31, 2011

Revised: December 2, 2011

Published: December 05, 2011

lipids⁹ and induce cross-ring cleavages in carbohydrate-based metabolites.¹⁰ The technique was demonstrated to cleave the S–S bond in Arg⁸-vasopressin, eliminating the need for wet chemistry prior to MS/MS analysis of peptides with strong disulfide bridges.¹¹ Finally, a study was conducted on *p*-nitrotoluene to compare the fs-LID MS/MS spectrum of the protonated parent ion with the fs-LID MS-TOF spectrum of the neutral molecule. Through careful pulse shaping methods, it was determined that transform limited femtosecond laser pulses are best in terms of efficiency for activation of the trapped ion population and protein structure determination does not require selective formation of certain product ions over others.¹¹

The most widely adopted approach for MS/MS experiments is collision induced dissociation (CID), whereby fragmentation is achieved through repeated collision of the precursor ions with helium atoms. The underlying dissociation process is well understood: as the energy gained through collisions is redistributed throughout the precursor ion, bond cleavage occurs according to bond dissociation energy. The most abundant product ions in the MS/MS spectrum are therefore those formed through the cleavage of the most labile bonds in the analyte. For peptides, the amino acid composition greatly influences the amenability of the molecule to protonation, the most likely protonation sites, and proton mobility in the gas phase. These factors can influence the observed dissociation patterns by enhancing cleavage of specific bonds.^{12,13} For example, peptide bonds are labile under mobile proton conditions as the backbone heteroatoms become protonated.¹⁴ This makes CID MS/MS spectra ideal for peptide sequencing when mobile protons are present, as a distribution of peptide bonds between each amino acid along the backbone chain dissociate. The mass-to-charge ratio of neighboring product ions in the sequence will differ by the mass of a single amino acid residue, meaning that the data can be used to reconstruct the sequence one amino acid at a time. However, this procedure is interrupted when unusually labile or nonlabile bonds are present that interfere with the standard dissociation patterns. Under nonmobile proton conditions where the proton or protons are sequestered at basic residues, the sequence coverage by CID is reduced.¹⁵ Nonlabile disulfide bonds between cysteine residues provide an additional obstacle to sequencing because they give some peptides a cyclic structure. This can be problematic because single peptide bond cleavages are not sufficient to fragment the ion, as the two pieces remain linked at the disulfide bridge. For this reason, peptide samples known to contain S–S bonds are often chemically reduced prior to MS/MS analysis by CID.¹⁶ This retains complete or nearly complete sequence coverage but loses important structural information related to sulfur–sulfur connectivity in the native structure. Alternatively, the presence of a labile chemical modification can interfere with peptide sequencing in a different manner. For example, during post-translational processing, a protein may become phosphorylated at a threonine, serine, or tyrosine residue as part of a cell signaling pathway. Under partially mobile or nonmobile proton conditions, the covalent bond between the phosphate group and the amino acid side chain is more labile than the backbone peptide bonds. The H-bonding character of the phosphate group allows for facile proton transfer from basic side chains, leading to a charge-directed loss of H₃PO₄.¹⁷ This means that upon activation by CID, the phosphate group or groups will be cleaved more readily than the peptide backbone, and the dominant product ion will reflect only this single cleavage, rather than a series of product ions for cleavages along the length of the peptide. Phosphate

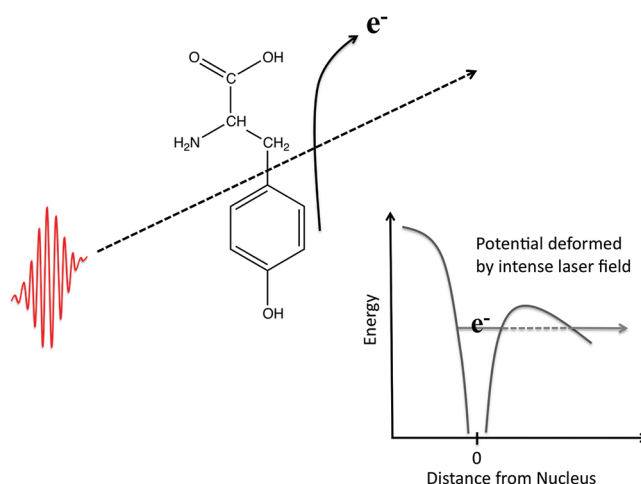


Figure 1. As an ultrafast laser pulse passes by the analyte, the intense electric field deforms the potential felt by electrons within the molecule. As a result, the electron that is most polarizable is able to escape from the analyte, leaving behind a photoionized radical site.

group loss and position scrambling have been identified as problematic in CID-MS studies.¹⁸

The branch of proteomics that focuses on post-translational modification (PTM) analysis is routinely faced with these more “problematic” samples, where comprehensive structural analysis requires the ability to cleave strong bonds while leaving more labile bonds intact. A number of alternative ion activation methods that are complementary to CID have been introduced to achieve this required nonthermal fragmentation. Electron capture dissociation (ECD)¹⁹ and electron transfer dissociation (ETD)^{20,21} activate the precursor ions through the formation of an unstable radical. The subsequent radical-directed fragmentation pathways cleave the peptide at different positions than CID, while leaving weakly bound PTMs intact. Photodissociation of trapped peptides in the ultraviolet^{22–26} and vacuum ultraviolet^{25,27–31} regimes also generate MS/MS spectra that are similar to ETD and ECD spectra and rely on photon absorption for ion activation rather than an electron source or electron transfer chemistry.^{31,32}

fs-LID is a viable alternative to these nonstatistical ion activation methods. fs-LID differs from other laser-induced activation methods in that the laser is in the near IR region, far from the electronic excitation transitions of peptides that are usually found in the UV spectral range. Although IR excitation often leads to thermal activation, intense femtosecond near-IR pulses can cause ultrafast electron loss through a process known as tunneling ionization.³³ The condition required to achieve tunneling ionization is that the electron must be able to acquire sufficient energy to overcome the binding energy within a single cycle of the optical field. This process is illustrated in Figure 1. For an excitation wavelength near 800 nm, this requires a peak power density of 10¹⁴ W/cm² and pulse duration shorter than 35 fs. These estimates are based upon reported ionization threshold values for small molecules in an intense laser field and have been generalized for larger molecules.^{34–36} Upon ionization of a protonated peptide, the oxidized species formed is a distonic cation $[M + H]^+ \rightarrow [M + H]^{2+*}$, which is susceptible to both proton- and radical-directed fragmentation pathways. As a result, fs-LID MS/MS spectra often contain a greater variety of product ions than observed in a CID spectrum alone. Though conservative predictions may expect product ion cleavages at or near the

original site of the radical, reactive radicals have actually been demonstrated to migrate upon formation within a peptide cation. This means that the radical is mobile and that its migration is coupled with rearrangements within the molecule.³⁷ This can give rise to backbone cleavages and side chain losses that propagate as far as five residues away from the initial radical site.^{38,39} This mechanism for ion activation is applicable to positive-mode MS/MS analysis of protonated peptides in any charge state and does not require a chromophore. fs-LID is compatible with any ion trap mass spectrometer, and the interfacing of the laser can be done without compromising the CID capability of the mass spectrometer. Currently, a large optical table is needed to support the amplified laser setup, but as ultrafast technology improves, the size and cost of these laser systems will decrease, making them more appealing to nonlaser experts. Ultimately, a compact femtosecond fiber laser system could be brought into an existing mass spectrometry facility, providing the option of fs-LID for routine daily MS/MS analyses. Novel approaches to fiber laser design, for example self-similar evolution⁴⁰ has allowed the development of compact fiber oscillators delivering peak power levels of 250 kW and 42 fs pulse duration.⁴¹

Photofragmentation studies of biomolecules using UV radiation from nanosecond lasers led to the suggestion that use of tunable fs-UV laser pulses might lead to efficient and nonergodic dissociation of large molecules.⁴² However, limited work has paired a femtosecond Ti:sapphire laser with an ion trap mass spectrometer for the dissociation of biomolecules. Laarman et al. used a learning algorithm with pulse shaping methods to optimize the cleavage of an acyl–N bond in Ac-Phe-NHMe to demonstrate the application of femtosecond pulse photodissociation for peptide sequencing.⁴³ Guyon et al. performed femtosecond pump–probe experiments on flavin, using the frequency doubled laser at 405 nm for resonant excitation of the inherent flavin chromophore.⁴⁴ Other experiments have interrogated the dissociation pathways of protonated aromatic amino acids and dipeptides using femtosecond pulses at 266 nm.^{45,46}

Here we present a bottom up analysis of the fragmentation mechanism involved in fs-LID tandem mass spectrometry. We start with the protonated amino acids and their derivatives to identify the most likely sites for laser–ion interaction. These trends are further supported by the fs-LID spectra for a series of small peptides containing single amino acid substitutions. Analysis of the fs-LID MS/MS spectra leads to the identification of principle cleavage pathways as well as some of the finer details of peptide dissociation by fs-LID.

2. EXPERIMENTAL METHODS

Experiments were conducted using a custom-built Quantronix (East Setauket, NY) Integra-HE amplified Ti:Al₂O₃ laser system. The broad-band output of the Ti-Light oscillator is passed through a 128-pixel MIIPS-enabled pulse shaper (Biophotonic Solutions Inc., East Lansing, MI) before seeding a 2-stage amplifier. The system is capable of delivering a 3.5 W output with a repetition rate of 10 kHz. The pulse-shaper is used to measure and compensate phase distortions accumulated as the laser beam passes through optics in the setup, resulting in transform-limited (TL) pulses with a ~26 nm (fwhm) bandwidth and ~35 fs duration at the sample.

L-Amino acids were purchased in a kit from Aldrich (St. Louis, MO) and prepared in a 50/50 water–methanol solution spiked with 1% acetic acid (MS buffer) at ~1 mg/mL concentration for

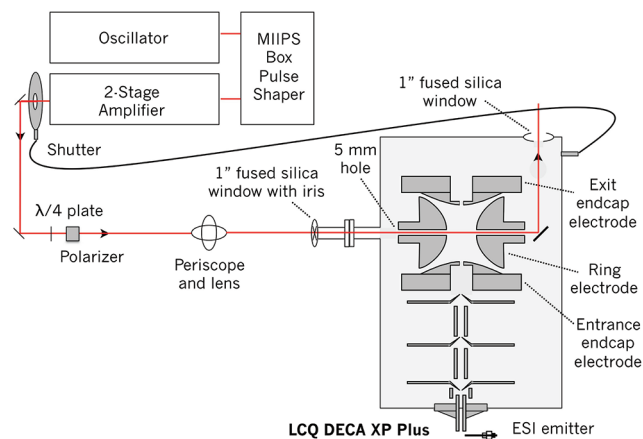


Figure 2. Instrumental setup of the amplified laser and 3D ion trap mass spectrometer.

direct analysis. Synthetic peptides were purchased from Auspep (Parkville, Australia) and GenScript Corp (Piscataway, NJ) and were also prepared in MS buffer at ~1 mg/mL.

The *N*-benzoyl derivatization was carried out as follows: 5 mg of each amino acid was dissolved in 200 μ L of 50 mM ammonium bicarbonate (pH 7.8), to which 100 μ L of benzoyl chloride was added and allowed to react for 2 h. Samples were dried and prepared in MS buffer at a ~1 mg/mL concentration.

The second derivatization scheme was an *N*-acetylation followed by methyl esterification of each amino acid. An acetylation reagent was prepared as 5 mL of acetic anhydride in 15 mL of methanol. Ten milligram samples of each amino acid were dissolved in 100 μ L of 50 mM NH₄HCO₃ and 1 mL of the acetylation reagent was added to each vial. Samples were well mixed and left to react at room temperature for 2 h before drying in the speed-vac. After drying, 1 mL of an esterification reagent (prepared by the dropwise addition of 800 μ L of acetyl chloride to 5 mL dry methanol on ice with constant stirring) was added to each sample vial and allowed to react at room temperature overnight. Samples were then dried, dissolved in MS buffer and diluted 50-fold for analysis. Note that without perfect conversion, many of the samples showed a mixture of the *N*-acetyl, methyl ester, and *N*-acetyl methyl ester derivatives upon MS analysis. The desired analyte was easily and cleanly separated from the byproducts during the isolation step in each MS/MS experiment.

All samples were subjected to electrospray ionization for introduction into a Thermo Finnigan LCQ Deca XP Plus ion trap mass spectrometer. The LCQ was modified in-house to accommodate laser irradiation of the trapped ion samples. A 1/2 in. diameter hole was drilled through the vacuum manifold in line with the ion trap, and a vacuum-sealed laser port was constructed with fused silica window. A 5 mm hole was drilled all the way through the ring electrode and the quartz spacers were notched accordingly to provide a clear path for the focused laser beam through the trap. Finally, a silver mirror was fixed to the vacuum manifold on the far side of the ion trap and used to direct the laser out another fused silica window in the back of the instrument. A manual flow controller was used to reoptimize the helium pressure within the trap following these structural modifications. A more detailed description of the modifications to the commercial mass spectrometer can be found elsewhere,⁶ and the setup is diagrammed in Figure 2. The beam from the Ti-light oscillator

passes through a MIIPS Box (Biophotonic Solutions Inc., East Lansing, MI) pulse shaper equipped with a 128-pixel spatial light modulator (SLM) before seeding the amplifier. A computer is used to control the voltages across each SLM pixel, whereby the phase across the bandwidth of the laser pulse can be altered. This technology allows us to measure and compensate for phase distortions, which cleans up the laser pulses and shortens the pulse duration of the amplified system from >70 fs to <40 fs. The fs-LID setup utilizes this ability to ensure that the femtosecond pulses are as short as possible (transform limited) when they reach the ion packet inside the 3D ion trap. Past experiments have shown that this is critical to fs-LID efficiency, as shown in Figure 3. The amplified laser beam is directed through a mechanical shutter, which is triggered to open and close when appropriate by the software that controls the mass spectrometer. A quarter wave plate and polarizer are used as a means of attenuating the amplified laser from the full 3.5 W output to an optimal fs-LID power. If the laser beam is too intense when it enters the vacuum manifold, the fs-LID signal-to-background ratio suffers. This trend as a function of laser power is shown in Figure 4 for a series of fs-LID spectra of protonated tryptophan. Finally, the amplified laser beam is directed up a periscope and focused through a lens before it enters the vacuum manifold via the fused silica window. Focusing the beam is necessary to pass the beam through the ion trap without hitting any of the metal surfaces, and it also provides a high peak power at the ion packet for ion activation. The unfocused beam (6.8×10^9 W/cm²) does not provide a peak power sufficient to initiate fs-LID; experiments indicate that a peak power on the order of 10^{13} W/cm² must be achieved before an fs-LID product ion signal is observed (data not shown).

For these experiments, the laser was attenuated to 1.2 W (120 μ J/pulse) and focused into the ion trap using a 600 mm focal length lens, resulting in a peak laser power of 7.5×10^{13} W/cm². Samples were isolated using the Advanced Define Scan panel of the LCQ Tune Plus software at a q -value of 0.25. To collect fs-LID data, the normalized collision energy was set to 0% and an

activation time of 100–200 ms was used. Note that the exposure time on the shutter control box has to be manually set to match the activation time to maximize the laser-ion packet interaction without exceeding the activation window and bombarding the dynode with photons as the product ions are being ejected to generate the MS/MS spectrum. Additionally, we chose to use a 3 microscan setting and average spectra over 3–5 min for each data file.

fs-LID data collection requires use of the built-in electronic triggering function to open and close the laser shutter during the appropriate ion activation step. To optimize our fs-LID signal before data collection, we adjust the ion trap fill time so that the isolation yields a precursor ion signal of approximately 10^6 counts. The automatic gain control can be used to do this, or

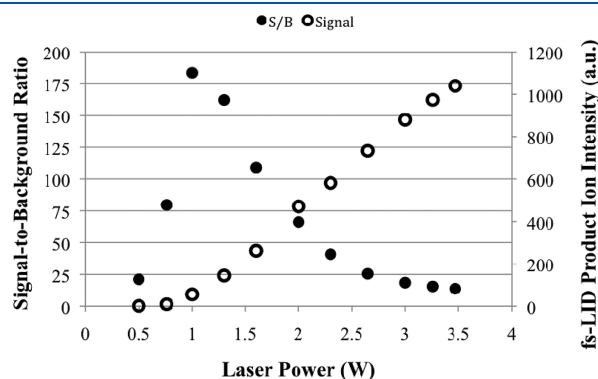


Figure 4. The intensity of the most abundant product ion in the fs-LID spectrum of protonated tryptophan ($[W+H]^+$) was monitored as a function of laser power (open circles). When the laser is allowed to irradiate a blank sample containing only MS buffer, certain unidentified peaks are observed, most of which lie below 300 m/z (not shown). The most intense such peak observed in the $[W+H]^+$ fs-LID spectrum at 77.1 m/z was also monitored as a function of laser power. The ratio of the product ion to the 77.1 m/z ion is presented here as the signal-to-background ratio (closed circles).

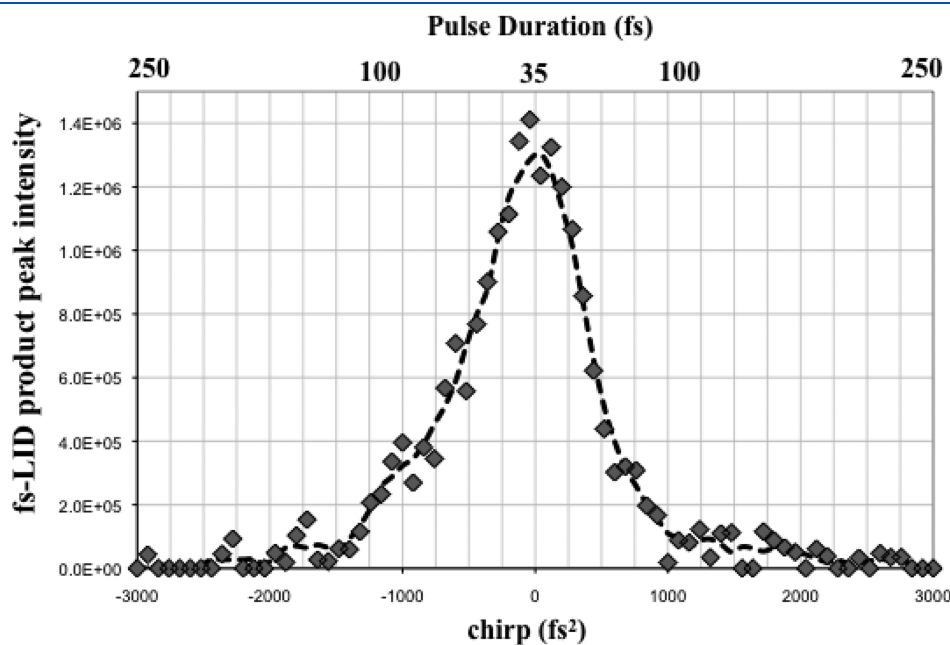


Figure 3. Short pulses are critical to fs-LID. Transform limited pulses with a duration of 35 fs maximize the intensity of the fs-LID product ion signal, whereas pulses that are stretched to 100 fs in duration result in a 80% loss of signal intensity.

the fill time can be set manually. We also tweak the laser beam angle slightly off of the top periscope mirror while monitoring the photoionization product ion peak using the manual tune window. When this peak is maximized, we know we are getting the maximum laser-ion packet overlap and therefore see the best fs-LID efficiency. This slight steering of the mirror is only necessary when switching between samples that differ significantly (>100 Da) in mass-to-charge ratio. This is likely because the ion packets are different sizes or the ion trajectories shift for precursor ions of different masses. Finally, note that fs-LID is a nonresonant ion activation method, so no wavelength tuning is necessary, nor do we modify our samples with chromophores.

3. RESULTS

The fragmentation reactions of the protonated α -amino acids by CID have been described in detail, with losses of NH_3 , H_2O , and $\text{H}_2\text{O} + \text{CO}$ being most common.⁴⁷ fs-LID does not yield the small molecule losses observed with CID. Without derivatization, the only protonated amino acids that give rise to an fs-LID signal are methionine, phenylalanine, tryptophan, and tyrosine (Table 1). These amino acids have the lowest ionization energies, which is consistent with the proposed photoionization mechanism for ion activation by fs-LID. However, Figure 5 reveals that ionization energy is not the sole predictor of fs-LID efficiency. Protonated phenylalanine gives rise to a more intense fs-LID signal than protonated methionine despite having higher ionization energy, suggesting that polarizability of the precursor ions is critical to ion activation by fs-LID.

The CID and fs-LID MS/MS spectra for protonated tyrosine are compared in Figure 6. As expected, the loss of NH_3 leads to

the base peak observed in the CID spectrum, and $\text{H}_2\text{O} + \text{CO}$ losses are also observed. The same $\text{H}_2\text{O} + \text{CO}$ loss is observed following activation by fs-LID, but dissociation appears to proceed through the photoionized intermediate $[\text{Y} + \text{H}]^{2+\bullet}$, as confirmed by the MS^3 spectrum shown in the bottom panel. NH_3 loss is absent in the fs-LID MS/MS spectrum and $\text{C}_{\alpha}-\text{C}_{\beta}$ bond dissociation gives rise to the $\text{C}_7\text{H}_7\text{O}^+$ product ion, which was not observed in the CID spectrum. Clearly, the two ion activation methods access different dissociation pathways.

On the basis of the results above, indicating that the presence of an aromatic ring enhances fs-LID activation, we evaluated all the amino acids after *N*-benzoyl derivatization. The presence of the benzoyl group led to a greater number of amino acids

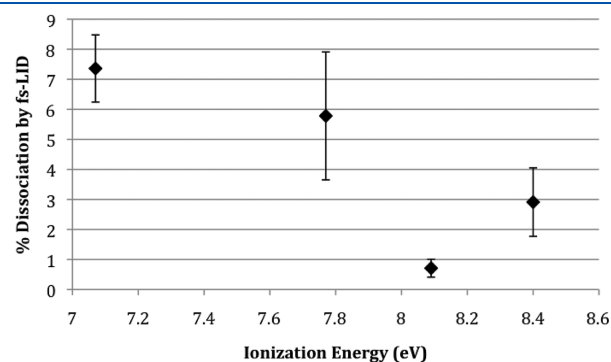


Figure 5. 90% confidence intervals of the mean fs-LID dissociation efficiency for protonated tryptophan, tyrosine, methionine, and phenylalanine (in that order) sorted by ionization energy from Table 1. Each confidence interval is based on 4–9 replicate measurements.

Table 1. Presence (Yes) or Absence (No) of fs-LID Signal Designated for Each Amino Acid in the Protonated $[\text{M} + \text{H}]^+$ Form as Well as the *N*-Benzoyl and *N*-Acetyl Methyl Ester Derivatives^a

amino acid	IE of neutral (eV) ⁴⁸	$[\text{M} + \text{H}]^+$	<i>N</i> -benzoyl	<i>N</i> -acetyl methyl ester
A - alanine	9.67 (NIST: 8.88)	no	no	no
C1 - L-cystine		no	no	yes
C2 - cysteine	8.66 (NIST: 9–9.5)	no	no	yes
D - aspartic acid	10.08	no		no
E - glutamic acid		no	no	no
F - phenylalanine	8.40	yes	yes	yes
G - glycine	9.82 (NIST ~ 9.2)	no	no	no
H - histidine	7.76/8.34	no	no	no
I - isoleucine	9.45 (NIST: 9.5)	no	no	yes
K - Lysine	8.98 (NIST: 8.6–9.5)	no	no	yes
L - leucine	9.51 (NIST: 8.51)	no	yes	yes
M - methionine	8.09 (NIST: 8.3–9.0)	yes	yes	yes
N - asparagine	9.31	no	yes	no
P1 - L-proline	8.75 (NIST: 8.3–9.3)	no	yes	yes
P2 - 4-hydroxy-L-proline	(NIST: 9.1)	no	yes	no
Q - glutamine		no	no	no
R - arginine	8.46	no	yes	no
S - serine	9.99 (NIST: 8.7–10)	no	yes	no
T - threonine	9.80 (NIST: < 10.2)	no	yes	no
V - valine	9.50 (NIST: 8.71)	no	no	no
W - tryptophan	7.07 (NIST: < 7.5)	yes	yes	yes
Y - tyrosine	7.77 (NIST: < 8.4)	yes	yes	yes

^a The calculated vertical ionization energies for several of the neutral amino acids in their low-lying conformations are reported,⁴⁸ and experimental values from the NIST Chemistry Webbook are reported where possible.

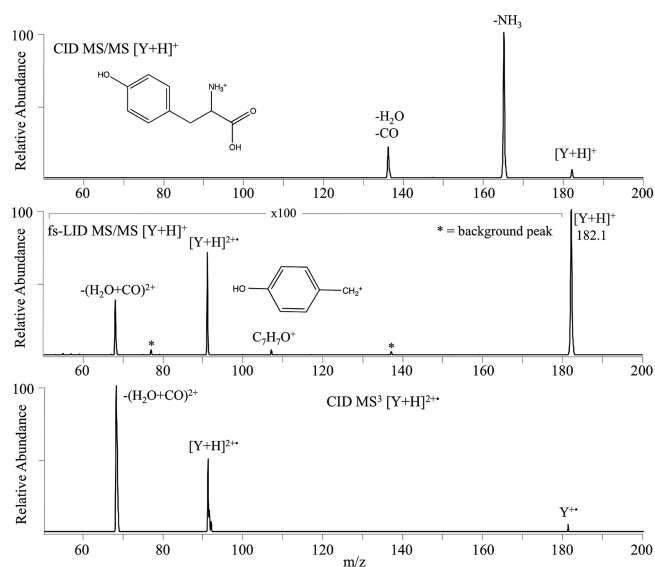


Figure 6. CID (top) and fs-LID (middle) spectra for protonated tyrosine illustrate the difference in dissociation pathways achieved by the two ion activation methods. CID MS³ of the photoionization product (lower panel) indicates that H₂O + CO loss proceeds through thermal excitation of the radical intermediate species.

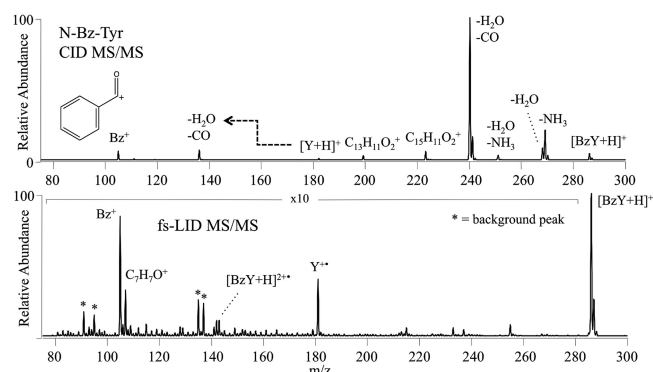


Figure 7. CID (top) and fs-LID (bottom) MS/MS spectra of *N*-benzoyl tyrosine. Note that NH₃ loss and minor product ions C₁₃H₁₁O₂⁺ and C₁₃H₁₁O₂⁺ in the CID spectrum indicate the presence of an isomeric impurity with the benzoyl addition occurring at the tyrosine side chain rather than the amine.

showing fs-LID ion activation events (Table 1). The CID and fs-LID MS/MS spectra for *N*-benzoyl tyrosine are compared in Figure 7. Once again, neutral losses dominate the CID spectrum whereas fs-LID ion activation proceeds through a radical intermediate. The photoionized [BzY + H]^{2+•} product ion is observed, as well as Bz⁺ and Y⁺, suggesting that the benzoyl group is a likely site of radical formation that leads to a radical-directed dissociation of the benzoyl group from the tyrosine molecule.

We also evaluated *N*-acetyl methyl ester derivatized amino acids. This derivatization was intended to simply lengthen the amino acid, without the addition of a highly polarizable group. The CID and fs-LID MS/MS spectra for *N*-acetyl tyrosine methyl ester are shown in Figure 8. The methyl ester and acetyl groups give rise to losses of CH₃OH, CH₃OH + CO, and CH₂CO following activation by CID, but these chemical modifications remain intact when ion activation is performed by fs-LID. The same

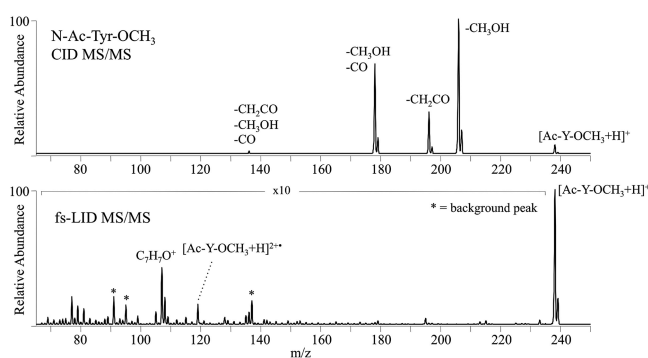


Figure 8. CID (top) and fs-LID (bottom) MS/MS spectra of the *N*-acetyl methyl ester tyrosine derivative.

C₇H₇O⁺ fs-LID product ion is observed here as was seen for the other tyrosine-based precursors in Figures 6 and 7.

Interestingly, between the two derivatization methods, we observed greater susceptibility to fs-LID for all amino acids except alanine, aspartic acid, glutamic acid, glycine, histidine, glutamine, and valine, as summarized in Table 1.

For a majority of the samples, the only product ion peak in the fs-LID MS/MS spectrum was the photoionization product, [M + H]^{2+•}. However, the samples with the lowest ionization energies did demonstrate limited bond dissociation, primarily at the C_α–C_β bond. The series of spectra for the tyrosine samples provided in Figures 6–8 are representative of the data for phenylalanine, methionine, and tryptophan. The photoionization product is observed in all three fs-LID MS/MS spectra, as is the C₇H₇O⁺ product ion, which corresponds to the tyrosine side chain after cleavage of the C_α–C_β bond. Neutral losses of small molecules such as NH₃, H₂O, CO, CH₃OH, and CH₂CO dominate the CID spectra of these samples, but these thermal dissociation pathways are mitigated in fs-LID. These samples illustrate that fs-LID is complementary to CID, and that fs-LID spectra are rich in structural information, as the nonergodic dissociation pathways lead to diagnostic product ions that are unique to the amino acid(s) in the sample, rather than a series of small molecule losses that could be observed from any amino acid.

4. DISCUSSION

4.1. Preliminaries. The transition from multiphoton ionization (MPI) to tunneling ionization was studied in atoms by Mevel et al. who noted that distinct features in the photoelectron spectra, separated by the photon energy $h\nu$ and associated with MPI, gradually disappear as the tunneling ionization becomes dominant.⁴⁹ A similar study was carried out on large polyatomic molecules (benzene, naphthalene, and anthracene), for which a broad featureless photoelectron spectrum was observed, stretching up to 25 eV.⁵⁰ The larger the molecule, the smoother the spectrum, indicating the dominant tunneling ionization features associated with above threshold ionization. The conditions of that study were (10¹³ W/cm², 780 nm, 170 fs). On the basis of those observations, the conditions in our experiment (larger molecules and much shorter pulses) support our designation of the activation event as tunneling ionization. Note that during tunneling ionization the molecule may acquire energy equivalent to that of tens of photons.

The fs-LID process is initiated by tunneling ionization of the most labile electron(s) in the molecule, and it leads to the

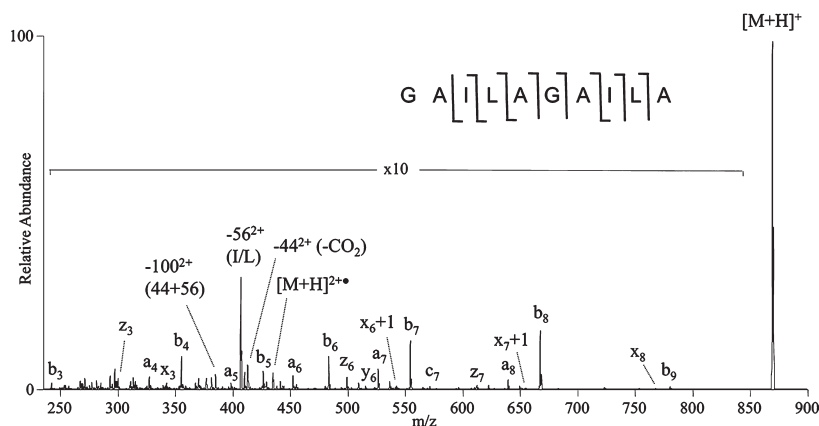


Figure 9. fs-LID MS/MS spectrum for GAILAGAILA.

formation of a radical cation. If no additional energy is deposited, the radical cation would fragment on a time scale long enough for intramolecular energy randomization, leading to statistical bond breakage. Based on extensive experimental data, bond dissociation occurring in fs-LID is nonergodic, suggesting that subsequent fragmentation occurs on a femtosecond time scale. We rationalize this by observing that the strong field acts on the entire macromolecule, pulling on most of the electrons. Although usually only one electron is lost, one can assume that many other electrons are strongly perturbed by the field. This leads to energy being deposited on the macromolecule. This energy manifests as multiple bond breaking events recorded as a series of product ions for a particular peptide. The total energy deposited by the strong field on a typical singly protonated peptide can be estimated by adding the ionization energy (10.9 eV)⁷ to the energy required to break one bond (4 eV) giving a total of ~ 15 eV or ~ 1450 kJ/mol. This amount of energy leads to ultrafast bond breaking. A more detailed analysis of the fs-LID process from single amino acids to peptides is given below.

4.2. Aromatics. Phenylalanine, tyrosine, and tryptophan all have ionization energies in the 7–8.5 eV range⁴⁸ and photoionize easily by fs-LID in both the protonated and derivatized forms. Although the delocalized π bonding electrons stabilize the resulting radical, we do observe significant radical-directed cleavage of the $C_\alpha-C_\beta$ bonds in all three amino acids, giving rise to a singly charged product ion corresponding to the mass of the amino acid's side chain. The other major product in these fs-LID spectra is a doubly charged product ion that has lost neutral CO_2 from the carboxylic acid end of the molecule. Based on our observations, the aromatic amino acids are the most likely sites for radical formation when a peptide is subjected to fs-LID.

4.3. Acidic/Basic Amino Acids. Aspartic acid and glutamic acid show no ionization or dissociation into product ions via fs-LID, regardless of derivatization, which is consistent with their high (~ 10 eV) ionization energy. Histidine also gives rise to no fs-LID product ions, which is surprising given the low (~ 8 eV) estimated ionization energy of the neutral form. Most likely, protonation of the histidine side chain is interfering with the conjugated pi system of electrons, making them less polarizable and therefore less susceptible to strong field ionization.

Lysine and arginine show limited degrees of photoionization by fs-LID only after derivatization as an *N*-acetyl methyl ester and *N*-benzoyl derivative, respectively. Because the side chains of these residues are basic, they are probable sites of protonation,

Table 2. Observed fs-LID Dissociation Efficiencies (%) for a Series of 12 Synthetic Peptides with Sequence GAIL(X1)GAIL(X2)^a

X2	X1			
	A	C	D	M
A	18.4	22.0	22.7	23.1
K	22.6	23.7	29.8	31.4
R	25.8	30.9	33.5	39.8

^a Efficiencies were calculated from the ratio of precursor ion abundances (normalized by the total ion current) in isolation and fs-LID spectra for each sample. Spectra for the samples of the three bold efficiencies can be found in Figures 9–11.

leaving few lone pair electrons susceptible to photoionization. Overall, the acidic and basic amino acids are unlikely origins for radical formation.

4.4. Polar Amino Acids. Glycine does not photoionize in any form, which is not surprising given that the hydrogen atom side chain does not enhance the polarizability of the amino acid backbone. More surprisingly, glutamine and its derivatives showed no fs-LID product ions, whereas asparagine gave rise to a small signal as an *N*-benzoyl derivative, as did serine and threonine. Though the interactions of the benzoyl group with the backbone of each amino acid and the resulting stereochemistry are unique, the aromatic group does increase the polarizability of some of these previously inactive polar amino acids to the point that fs-LID signal can be observed. The bulky benzoyl group did not improve the amenability of cystine or cysteine to fs-LID, but a simple lengthening of the backbone in the *N*-acetyl methyl ester forms was sufficient to observe limited photoionization.

4.5. Nonpolar Amino Acids. The susceptibility to fs-LID of the nonpolar amino acids was found to increase with size and therefore polarizability. Alanine and valine were completely inactive, whereas leucine, isoleucine, and proline could be photoionized upon derivatization (Table 1). Methionine is the exception in this category; the S heteroatom in the side chain significantly lowers the ionization energy and accordingly, and the activated sample gives rise to strong fs-LID product ions in all protonated and derivatized forms.

The fs-LID MS/MS analysis of single amino acids allowed us to elucidate the most likely origin of the $[M+H]^{2+\bullet}$ ion-radical pair. Methionine and the aromatic residues are the most amenable

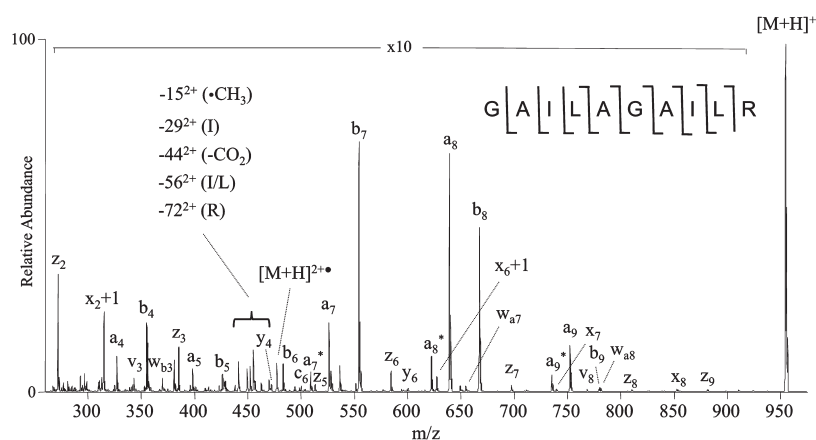


Figure 10. fs-LID MS/MS spectrum for GAILAGAILR.

to photoionization. Extending to slightly larger molecular systems, the fs-LID product ion signal seems to track with ionization potential or polarizability. Utilizing the benzoyl group as a chromophore was one successful method for generating fs-LID product ions from previously inactive samples. However, this sort of wet chemistry is unnecessary if the analyte is sufficiently large. The *N*-acetyl methyl ester derivatives were studied to mimic the lengthening of the backbone in a longer peptide or protein, and this modification also led to the observation of fs-LID product ions from previously inactive amino acids. Our conclusion is that longer peptides will be largely amenable to interrogation by fs-LID regardless of their sequence, without the need for any derivatization prior to MS/MS analysis.

4.6. Extension to Peptides. In proteomic MS/MS, the greater the number of assignable product ions observed, the more information-rich the spectrum can be considered. Peptide sequencing can be done manually or with the aid of software, whereby pairs of peaks that differ by the mass of a single amino acid are used to map out the identity and order of residues in the precursor sequence. If a specific region of the peptide does not fragment well, the exact sequence cannot be assigned. Although some of the product ions corresponding to backbone cleavages may be redundant (in that we observe multiple cleavages between the same pair of residues), they increase our confidence in the ultimate sequence assignment. Therefore, it is advantageous to find an ion activation method that yields a greater variety of product ions, rather than simply a high intensity of product ions.

The robustness of fs-LID as an ion activation method is confirmed by the fs-LID spectrum of the peptide GAILAGAILA, which contains no aromatic or methionine residues (Figure 9). The polarizability of the large molecule is sufficient for photoionization and gives rise to sufficient product ions for nearly 100% sequence coverage. The most abundant product ions are the -56^{2+} (side chain loss from Leu or Ile) and a nearly complete series of b-ions, limited only by the low mass cutoff (LMCO) associated with isolation of the precursor at 869.4 Da.

A single residue substitution at the C-terminal end of the peptide from alanine to arginine leads to a $\sim 7\%$ increase in dissociation efficiency by fs-LID (Table 2) and also gives rise to more abundant a-ions near the C-terminal end of the GAILAGAILR peptide (Figure 10). This suggests that photoionization of the precursor occurs predominantly at the arginine residue. The -72^{2+} product ion corresponds to partial loss of the arginine side chain as a radical following cleavage of the $C_\beta-C_\gamma$ bond

Table 3. Observed fs-LID Side Chain Losses from Residues in the GAIL(X1)GAIL(X2) Series

residue	mass of side chain loss (Da)	chemical formula
C	33	SH
D	44	CO ₂
I	29, 56 (Figures 9–11)	\bullet C ₂ H ₅ , C ₄ H ₈
K	72	\bullet C ₄ H ₁₀ N
L	43, 56 (Figures 9–11)	\bullet C ₃ H ₇ , C ₄ H ₈
M	61, 74 (Figure 11)	\bullet C ₂ H ₅ S, C ₃ H ₆ S
R	72, 100 (Figures 10 and 11)	\bullet C ₂ H ₆ N ₃ , C ₄ H ₁₀ N ₃ ⁺

whereas the rest of the peptide remains intact. Another notable feature in the fs-LID spectrum is the presence of satellite ions v_3 , w_{b3} , w_{a7} , v_8 , and w_{a8} , which can be used to differentiate between Ile and Leu residues when the peptide is sequenced.

Alternatively, we can seed a likely origin for the radical into the peptide with a single residue substitution that places a methionine residue in the fifth position. This dramatically increases the fs-LID dissociation efficiency to nearly 40% as shown in Table 2. This was expected given the fs-LID activity of protonated methionine observed earlier. Note that the fs-LID spectrum of GAILMGAILR (Figure 11) has a base peak of $[M + H]^{2+}$ due to the stability of the radical formed at the methionine residue. This stability not only detracts slightly from the abundance of sequence ions but also gives rise to strong side chain losses from methionine, -61^{2+} and -74^{2+} , that can be used as diagnostic indicators of methionine in unknown peptide or protein samples.

The diagnostic side chain losses observed in fs-LID spectra of 12 synthetic peptides have been tabulated in Table 3 and are consistent with those reported in the literature.^{38,39,51} Note that the neutral loss of even-electron species leaves a radical on the doubly charged peptide backbone and can give rise to sequence ions, meaning that many of the side chain losses observed in fs-LID are intermediate rather than “dead-end” product ions. This opens the door for sequential dissociation and also provides radical intermediates that can be isolated and subjected to MS³ (or MSⁿ) for further analysis when present in sufficient abundance. The side chain losses from I, L, M, and R can be seen in the fs-LID spectra as noted in Figures 9–11.

The fs-LID dissociation efficiencies for the three peptide samples discussed above are combined with those of nine similar

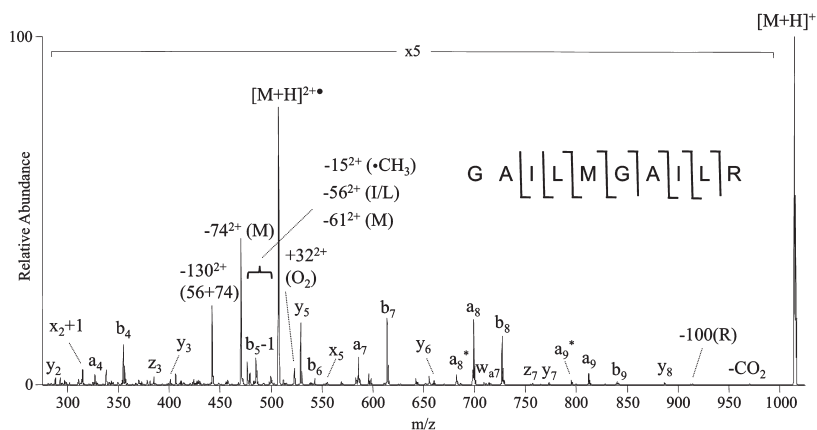


Figure 11. fs-LID MS/MS spectrum for GAILMGAILR.

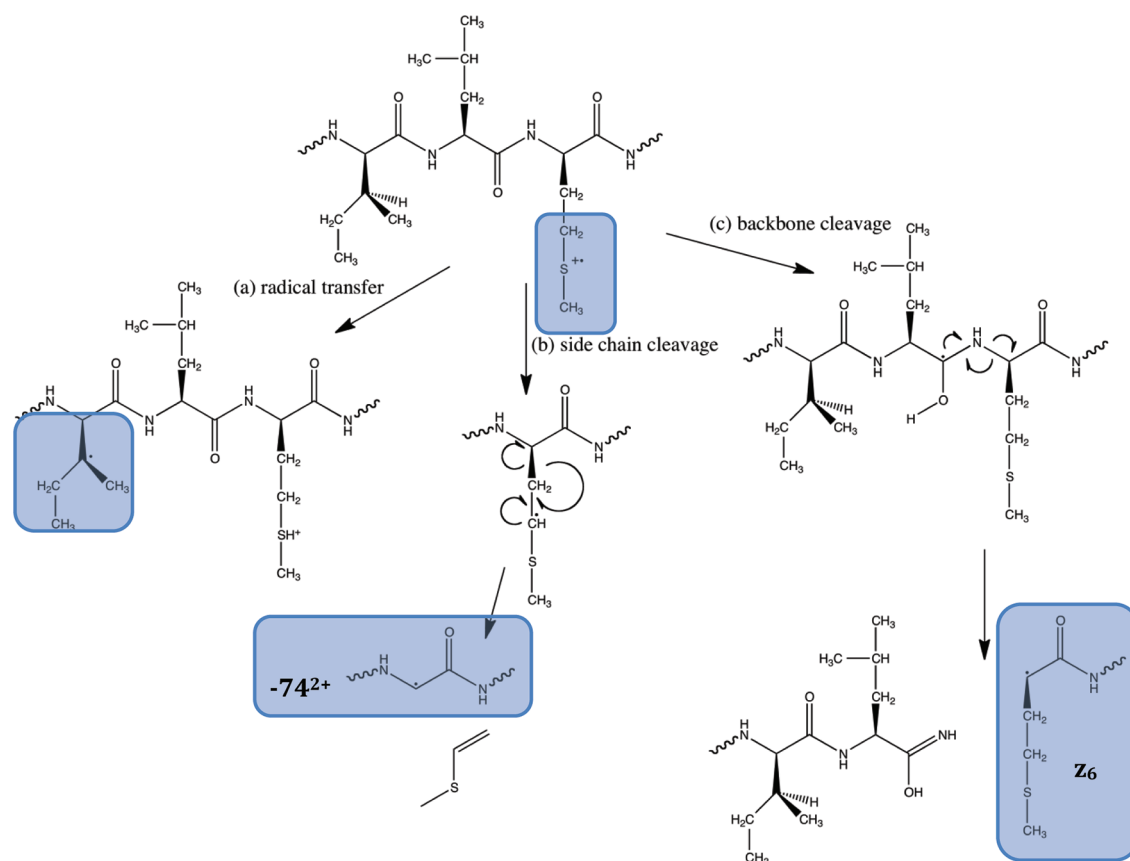


Figure 12. In the gas phase, the dionic species can dissociate via a number of pathways. The mechanisms shown here are meant to illustrate the variety of product ions that can form.

samples in Table 2. The peptide sequence is GAIL(X1)GAIL(X2) where X1 = alanine (A), cysteine (C), aspartic acid (D), or methionine (M) and X2 = alanine (A), lysine (K), or arginine (R). A two-way ANOVA test revealed that both the X1 effect and the X2 effect are statistically significant ($p = 0.0129$ and 0.0016 , respectively). As the X1 residue changes from A to C to D to M, the polarizability of the peptide increases. As X2 changes from A to K to R, the proton mobility of the peptide decreases. Polarizability and proton mobility are not completely independent nor easily quantifiable for these samples, so the interaction effects cannot be analyzed.

In general, if the peptide being analyzed contains one or more F, M, W, or Y residues, we expect to see the photoionized $[M + H]^{2+•}$ product as the base peak in the fs-LID MS/MS spectrum. In most other samples analyzed, products arising from side chain losses or sequence ions of type a and b are the most abundant, and all spectra contained a, b, x, y, and z-type ions. C-type sequence ions are the only product ions we do not observe regularly when using fs-LID for ion activation of these peptides. We also see an increase in sequence ion abundances near residues like C, K, and R, which have moderate ionization energies and are potential sites for side chain losses.

Depending on the nature of the original radical site, H⁺ or H[•] abstraction is likely to follow to stabilize the radical. If the hydrogen comes from a side chain, the result is either a side chain loss or propagation of the radical along the peptide chain. H[•] transfer to a carbonyl along the peptide backbone as well as proton-driven chemistry will occur at the same time to produce sequence ions. A possible mechanism for each case is outlined in Figure 12. In Figure 12, the ILM portion of the GAILMGAILR peptide is shown after undergoing photoionization. The radical is shown at its most likely origin, the S atom of the methionine side chain. Pathway (a) illustrates a possible H[•] transfer that results in the radical position migrating two side chains down the peptide backbone to the C_β atom on the isoleucine side chain. This intermediate would then contribute to the −56²⁺ product ion intensity observed in Figure 11. Pathway (b) follows the radical-directed cleavage of the C_α–C_β bond in the methionine side chain, resulting in the neutral loss of 74 Da, corresponding to the −74²⁺ product ion peak in Figure 11. Finally, pathway (c) illustrates one possible outcome of the radical migrating away from the methionine side chain. The ion can now undergo a radical-directed backbone cleavage of the N–C_α bond in the peptide, resulting in c and/or z-type ions. Note that this mechanism is not specific to methionine and could occur at various points along the peptide, giving rise to the z₃ and z₇ ions observed in Figure 11. The mechanism is shown at the methionine residue here only for simplicity; in reality the resulting z₆ ion is a minor product ion and is not labeled in the spectrum shown in Figure 11.

5. CONCLUSION

Overall, fs-LID has been shown to generate information-rich MS/MS spectra. Through the analysis of protonated amino acids, we have identified the aromatic amino acids and methionine as the most likely sites of radical formation upon tunnel ionization and have determined that ionization energy is not the sole predictor of sample amenability to fs-LID. As the fs-LID MS/MS spectra of the peptides illustrate, high polarizability and low proton mobility can boost fs-LID dissociation efficiency up above 35%, even in samples with no aromatic chromophore to enhance ion activation. This makes fs-LID an attractive ion activation technique because it requires no chromophore or sample derivatization prior to MS/MS analysis. Whereas a VUV laser can be used to photodissociate peptides due to the absorption maximum of peptide bonds around 190 nm,⁵² a femtosecond laser can activate any class of molecules via tunneling ionization, independent of their absorption spectra.

Another benefit of fs-LID is that it creates a radical to access several nonergodic dissociation pathways. A majority of this gas phase radical chemistry has been studied using electron capture or electron transfer dissociation (ECD/ETD), which reduces multiply charged gas phase ions to form hydrogen-abundant radical cations ([M + 2H]²⁺ → [M + 2H]^{•+}). By comparison, fs-LID intermediates are hydrogen-deficient ([M + H]⁺ → [M + H]^{2+•}), and therefore the technique does not need a multiply charged precursor to carry out ion activation in positive ion mode. This makes fs-LID appropriate for pairing with MALDI sources, as the soft ionization method is known to generate singly protonated ions. Preliminary studies on negative ion mode using fs-LID have also shown promising results and higher product ion yields, indicating that fs-LID may one day be appropriate for high throughput proteomic and metabolomic studies.

ACKNOWLEDGMENT

The instrument used for this study was funded by grant 156 of the 21st Century Jobs Trust Fund of the SEIC Board from the State of Michigan. Additional support comes from grant CRIF ID 0923957 from the National Science Foundation. CLK acknowledges support from an NSF Graduate Research Fellowship.

REFERENCES

- (1) Fenn, J. B.; Mann, M.; Meng, C. K.; Wong, S. F.; Whitehouse, C. M. *Science* **1989**, *246*, 64.
- (2) Hillenkamp, F.; Karas, M.; Beavis, R. C.; Chait, B. T. *Anal. Chem.* **1991**, *63*, A1193.
- (3) Yates, J. R. *J. Mass Spectrom.* **1998**, *33*, 1.
- (4) Sleno, L.; Volmer, D. A. *J. Mass Spectrom.* **2004**, *39*, 1091.
- (5) Wysocki, V. H.; Resing, K. A.; Zhang, Q. F.; Cheng, G. L. *Methods* **2005**, *35*, 211.
- (6) Kalcic, C. L.; Gunaratne, T. C.; Jonest, A. D.; Dantus, M.; Reid, G. E. *J. Am. Chem. Soc.* **2009**, *131*, 940.
- (7) Budnik, B. A.; Tsybin, Y. O.; Hakansson, P.; Zubarev, R. A. *J. Mass Spectrom.* **2002**, *37*, 1141.
- (8) Smith, S. A.; Kalcic, C. L.; Safran, K. A.; Stemmer, P. M.; Dantus, M.; Reid, G. E. *J. Am. Soc. Mass Spectrom.* **2010**, *21*, 2031.
- (9) Smith, S. A.; Kalcic, C. L.; Dantus, M.; Reid, G. E. *Phospholipid Analysis by Femtosecond Laser-Induced Ionization/Dissociation Mass Spectrometry (fs-LID MS)*. *57th ASMS Conference*, 2009.
- (10) Winkler, N. S.; Kalcic, C. L.; Jones, A. D.; Dantus, M. *Study of metabolites including alpha-tomatine by femtosecond laser-induced ionization/dissociation (fs-LID)*. *57th ASMS Conference*, 2009.
- (11) Zhu, X.; Kalcic, C. L.; Winkler, N.; Lozovoy, V. V.; Dantus, M. *J. Phys. Chem. A* **2010**, *114*, 10380.
- (12) Dongre, A. R.; Jones, J. L.; Somogyi, A.; Wysocki, V. H. *J. Am. Chem. Soc.* **1996**, *118*, 8365.
- (13) Kapp, E. A.; Schatz, F.; Reid, G. E.; Eddes, J. S.; Moritz, R. L.; O'Hair, R. A. J.; Speed, T. P.; Simpson, R. J. *Anal. Chem.* **2003**, *75*, 6251.
- (14) Wysocki, V. H.; Tsapralis, G.; Smith, L. L.; Brechi, L. A. *J. Mass Spectrom.* **2000**, *35*, 1399.
- (15) Pu, D.; Clipston, N. L.; Cassady, C. J. *J. Mass Spectrom.* **2010**, *45*, 297.
- (16) Gorman, J. J.; Wallis, T. P.; Pitt, J. J. *Mass Spectrom. Rev.* **2002**, *21*, 183.
- (17) Palumbo, A. M.; Tepe, J. J.; Reid, G. E. *J. Proteome Res.* **2008**, *7*, 771.
- (18) Palumbo, A. M.; Reid, G. E. *Anal. Chem.* **2008**, *80*, 9735.
- (19) Zubarev, R. A.; Horn, D. M.; Fridriksson, E. K.; Kelleher, N. L.; Kruger, N. A.; Lewis, M. A.; Carpenter, B. K.; McLafferty, F. W. *Anal. Chem.* **2000**, *72*, 563.
- (20) Mikesch, L. M.; Ueberheide, B.; Chi, A.; Coon, J. J.; Syka, J. E. P.; Shabanowitz, J.; Hunt, D. F. *Biochim. Biophys. Acta* **2006**, *1764*, 1811.
- (21) Wiesner, J.; Premsler, T.; Sickmann, A. *Proteomics* **2008**, *8*, 4466.
- (22) Wilson, J. J.; Brodbelt, J. S. *Anal. Chem.* **2007**, *79*, 7883.
- (23) Wilson, J. J.; Kirkovits, G. J.; Sessler, J. L.; Brodbelt, J. S. *J. Am. Soc. Mass Spectrom.* **2008**, *19*, 257.
- (24) Joly, L.; Antoine, R.; Broyer, M.; Dugourd, P.; Lemoine, J. *J. Mass Spectrom.* **2007**, *42*, 818.
- (25) Yoon, S. H.; Chung, Y. J.; Kim, M. S. *J. Am. Soc. Mass Spectrom.* **2008**, *19*, 645.
- (26) Perot, M.; Lucas, B.; Barat, M.; Fayeton, J. A.; Jouvet, C. *J. Phys. Chem. A* **2010**, *114*, 3147.
- (27) Kim, T. Y.; Reilly, J. P. *J. Am. Soc. Mass Spectrom.* **2009**, *20*, 2334.
- (28) Parthasarathi, R.; He, Y.; Reilly, J. P.; Raghavachari, K. *J. Am. Chem. Soc.* **2010**, *132*, 1606.
- (29) Madsen, J. A.; Boutz, D. R.; Brodbelt, J. S. *J. Proteome Res.* **2010**, *9*, 4205.
- (30) Madsen, J. A.; Kaoud, T. S.; Dalby, K. N.; Brodbelt, J. S. *Proteomics* **2011**, *11*, 1329.

- (31) Cui, W. D.; Thompson, M. S.; Reilly, J. P. *J. Am. Soc. Mass Spectrom.* **2005**, *16*, 1384.
- (32) Reilly, J. P. *Mass Spectrom. Rev.* **2009**, *28*, 425.
- (33) Posthumus, J. H. *Rep. Prog. Phys.* **2004**, *67*, 623.
- (34) Lozovoy, V. V.; Zhu, X.; Gunaratne, T. C.; Harris, D. A.; Shane, J. C.; Dantus, M. *J. Phys. Chem. A* **2008**, *112*, 3789.
- (35) Hankin, S. M.; Villeneuve, D. M.; Corkum, P. B.; Rayner, D. M. *Phys. Rev. A* **2001**, *64*, 013405.
- (36) Uiterwaal, C.; Gebhardt, C. R.; Schroder, H.; Kompa, K. L. *Eur. Phys. J. D* **2004**, *30*, 379.
- (37) Moore, B. N.; Blanksby, S. J.; Julian, R. R. *Chem. Commun.* **2009**, 5015.
- (38) Sun, Q. Y.; Nelson, H.; Ly, T.; Stoltz, B. M.; Julian, R. R. *J. Proteome Res.* **2009**, *8*, 958.
- (39) Savitski, M. M.; Nielsen, M. L.; Zubarev, R. A. *Anal. Chem.* **2007**, *79*, 2296.
- (40) Renninger, W. H.; Chong, A.; Wise, F. W. *Phys. Rev. A* **2010**, *82*, 021805.
- (41) Nie, B.; Pestov, D.; Wise, F. W.; Dantus, M. *Opt. Express* **2011**, *19*, 12074.
- (42) Jia, W. J.; Ledingham, K. W. D.; Scott, C. T. J.; Kosmidis, C.; Singhal, R. P. *Rapid Commun. Mass Spectrom.* **1996**, *10*, 1597.
- (43) Laarmann, T.; Shchatsinin, I.; Singh, P.; Zhavoronkov, N.; Gerhards, M.; Schulz, C. P.; Hertel, I. V. *J. Chem. Phys.* **2007**, *127*, 201101.
- (44) Guyon, L.; Tabarin, T.; Thuillier, B.; Antoine, R.; Broyer, M.; Boutou, V.; Wolf, J. P.; Dugourd, P. *J. Chem. Phys.* **2008**, *128*, 075103.
- (45) Kang, H.; Jouvét, C.; Dedonder-Lardeux, C.; Martrenchard, S.; Gregoire, G.; Desfrancois, C.; Schermann, J. P.; Barat, M.; Fayeton, J. A. *Phys. Chem. Chem. Phys.* **2005**, *7*, 394.
- (46) Gregoire, G.; Kang, H.; Dedonder-Lardeux, C.; Jouvét, C.; Desfrancois, C.; Onidas, D.; Lepere, V.; Fayeton, J. A. *Phys. Chem. Chem. Phys.* **2006**, *8*, 122.
- (47) Dookeran, N. N.; Yalcin, T.; Harrison, A. G. *J. Mass Spectrom.* **1996**, *31*, 500.
- (48) Dehareng, D.; Dive, G. *Int. J. Mol. Sci.* **2004**, *5*, 301.
- (49) Mevel, E.; Breger, P.; Trainham, R.; Petite, G.; Agostini, P.; Migus, A.; Chambaret, J. P.; Antonetti, A. *Phys. Rev. Lett.* **1993**, *70*, 406.
- (50) Levis, R. J.; DeWitt, M. J. *J. Phys. Chem. A* **1999**, *103*, 6493.
- (51) Laskin, J.; Yang, Z. B.; Ng, C. M. D.; Chu, I. K. *J. Am. Soc. Mass Spectrom.* **2010**, *21*, 511.
- (52) Goldfarb, A. R.; Saidel, L. J.; Mosovich, E. *J. Biol. Chem.* **1951**, *193*, 397.